

Compositional Analysis of Oxygenates and Hydrocarbons in Waste and Virgin Polyolefin Pyrolysis Oils by Ultrahigh-Resolution Fourier Transform Ion Cyclotron Resonance Mass Spectrometry

Yannick Ureel, Martha L. Chacón-Patiño, Marvin Kusenberg, Anton Ginzburg, Ryan P. Rodgers, Maarten K. Sabbe, and Kevin M. Van Geem*



Cite This: <https://doi.org/10.1021/acs.energyfuels.4c03835>



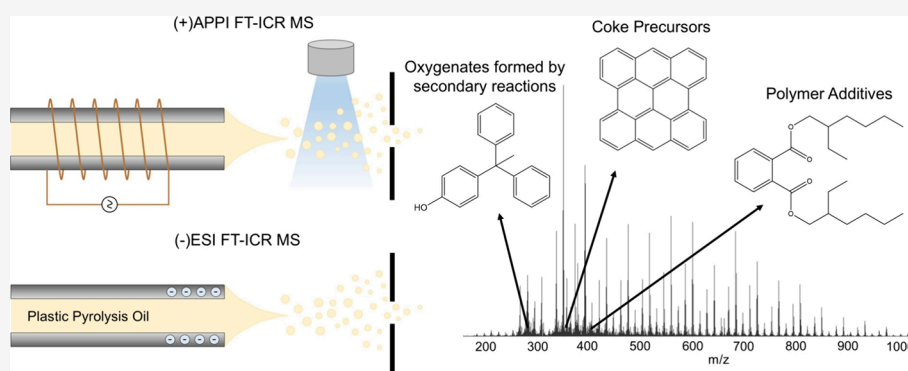
Read Online

ACCESS |

Metrics & More

Article Recommendations

Supporting Information



ABSTRACT: The linear plastic lifecycle is unsustainable. Mechanical recycling of mixed plastic waste remains challenging, making chemical recycling necessary. Polyolefins, the largest share of plastic waste, can be chemically recycled through thermal pyrolysis. However, the impact of the feedstock type on pyrolysis oil composition remains unclear. Only very advanced analytical techniques allow to assess the detailed composition of these oils, which is crucial to evaluate their economic potential. Therefore, in this work, the hydrocarbon and oxygenate contents of three pyrolysis oils derived from postconsumer waste polyethylene, polypropylene, mixed polyolefins, and virgin polyethylene are characterized by ultrahigh-resolution Fourier transform ion cyclotron resonance mass spectrometry. Both positive-ion atmospheric-pressure photoionization and negative electrospray ionization were employed to identify oxygenates and hydrocarbons. It was found that the presence of trace polymers, metals, and polymer defects in postconsumer waste oils resulted in a higher fraction of complex polycyclic aromatic hydrocarbons compared to virgin pyrolysis oils. Furthermore, clear sources of oxygenates (polymer additives, trace polymers, or organic residues) could be identified in all four samples. Suspected thermal dissociation products of polymer additives such as Irganox 1010 and diethylhexyl phthalate (DEHP) were observed, indicating the various reactions occurring upon pyrolysis of these complex blends. The fact that a variety of additive-derived contaminants were found in pyrolysis oil from virgin polyolefins further indicates that pyrolysis oil contaminants do not exclusively accumulate during the plastics' lifetime but could potentially be limited on the manufacturing side. This unprecedented level of molecular detail in the compositional analysis of plastic pyrolysis oils will aid in the development of improved recycling strategies, which can help close the loop to a circularized lifecycle for polyolefin waste.

1. INTRODUCTION

Around 10% of all fossil hydrocarbons are used for the production of plastics, corresponding to a production of 350 Mt annually.^{1,2} While plastics are an incredibly lightweight versatile material, their end-of-life is a huge burden on the environment.^{3,4} Globally, only 10% of the plastics in the world are recycled, with 19% being incinerated for energy recovery, and the majority ends up as landfill (49%) or is lost to the environment (22%).⁵ This linear plastic economy results in plastic pollution of the environment (e.g., the great Pacific garbage patch), a huge emission of greenhouse gases, and the need for fossil feedstocks to produce new polymers. By

transitioning from linear to a circular plastics economy, where end-of-life polymers are recycled to new materials in a closed loop, all three problems can be alleviated. While mechanical recycling has the largest carbon avoidance potential of all

Received: August 8, 2024

Revised: October 7, 2024

Accepted: October 9, 2024

recycling techniques, closed-loop recycling is challenging for heterogeneous polymer mixtures. Especially for polyolefins (polyethylene (PE) and polypropylene (PP)), closed-loop mechanical recycling is unfeasible, even though this waste stream accounts for 60% of plastic waste.⁶ Mechanical recycling suffers from three fallbacks: thermomechanical degradation, polymer immiscibility, and the presence of additives and waste contaminants.^{6,7} Mechanical recycling utilizes a principal thermoplastic character of the polymer, where it is brought back to the molten state and subjected to high shears during the reprocessing. This results in severe thermomechanical chain degradation, which yields products with deteriorated material properties. Furthermore, due to the very similar density, separation of PE and PP fractions via conventional sorting techniques such as sink-float separation is nearly impossible. Furthermore, removal of all the polymer additives present in the plastic waste is impossible with conventional techniques, resulting in a recycled product of inferior quality.⁸ Thus, a technique to improve the closed-loop recycling rates of polyolefin waste is hence chemical recycling in which the polymers are converted into chemical feedstocks, which can subsequently be used to produce new virgin-grade polymers. It is estimated that over 655 Mt CO₂ annually can be saved by chemical recycling of plastic waste compared to the current plastic end-of-life, corresponding to 1.87 t CO₂ per ton of recycled plastic.^{6,9} However, of the global 9% of recycled polymers, the majority are still mechanically recycled, while chemical recycling is almost entirely absent in the current recycling industry.¹

Thermal or catalytic pyrolysis of waste plastics is one of the most preferred options to recycle complex polyolefin waste fractions.^{10–12} During thermal pyrolysis of plastic waste, the plastics undergo cracking to produce pyrolysis oils. These oils are subsequently refined downstream into plastic monomers and other base chemicals through either steam or fluid catalytic cracking.^{13–15} With catalytic pyrolysis, the aim is to promote this cracking further either *in situ* or *ex situ*, to increase the fraction of valuable products.^{16,17} The produced plastic pyrolysis oils are a complex mixture of hydrocarbons, which contain contaminants comprising nearly the whole periodic system.^{18,19} These contaminants originate from polymer additives, traces of nonpolyolefinic polymers due to imperfect sorting, and organic waste accumulated during the lifetime of the plastics. The presence of contaminants hampers downstream processing of plastic pyrolysis oils in the current chemical industry.^{15,20} The heteroatoms present in the pyrolysis oils can induce coking and reduce the carbon efficiency in steam cracking and thermal pyrolysis. For example, an excessive presence of nitrogen, halogens, or metals will result in catalyst poisoning during fluid catalytic cracking or other downstream catalytic processes.^{21,22} The most abundant heteroatom in plastic pyrolysis oils is oxygen, which originates from various plastic additives, ill-sorted polymers, and organic residues.^{18,23} The oxygenates present in the plastic pyrolysis oil can react further with the hydrocarbon matrix resulting in various impurities upon further chemical processing. Moreover, when steam cracking the plastic pyrolysis oils, the oxygen present will primarily end up under the form of carbon dioxide and carbon monoxide.^{24,25} This production of carbon oxides decreases the carbon efficiency of the steam cracker, creates issues in the separation section, and thus makes the pyrolysis oil less valuable for the chemical industry.

The prevention of impurities in the plastic waste starts by thorough sorting and washing of the waste feed. The postconsumer plastic waste runs through several sorting and purification steps prior to recycling.^{3,26} This sorting comprises the removal of glass, metals, and other foreign materials based on size (sieves), magnetic properties (magnetic attraction or induced magnetic repulsion), or optical properties (infrared spectra).²⁶ Subsequently, the polymers can be separated further by various approaches based on gravity or optical properties. As the density of polymers differs depending on the polymer type (PP or PE, 900 kg m⁻³; PET or PVC, 1400 kg m⁻³), a sink-float separation can be employed by using water.²⁷ Furthermore, sorting based on infrared, ultraviolet, or X-rays is a potential strategy to refine these polymer streams further and reduce the fraction of contaminants. However, pure polyolefin streams are currently not achievable by sorting. Next to these mechanical strategies to improve the purity of the solid waste feedstock, different potential chemical decontamination methods of the obtained pyrolysis oil are known. For instance, techniques such as hydrotreating, dehalogenation, and membrane filtration exist today to decontaminate the produced pyrolysis oils.²⁸ Importantly, fundamental knowledge of the molecular compositions of the plastic pyrolysis oil and its contaminants is essential to determine the optimal decontamination strategy.

Several analytical techniques have been employed to examine the composition of plastic pyrolysis oils. Since these oils primarily consist of hydrocarbons, much research has been dedicated to elucidating the intricate hydrocarbon composition within these complex mixtures.^{29,30} The hydrocarbon matrix has been frequently investigated by one-dimensional gas chromatography (1DGC) coupled to various detectors; however, these techniques typically only allow identification of low-molecular-mass compounds and lump C₅₊ species.³¹ On the other hand, two-dimensional comprehensive gas chromatography (GC × GC) has become one of the most popular and efficient methods to determine the hydrocarbon composition of complex mixtures. Especially, GC × GC coupled to a flame ionization detector (GC × GC-FID) is valuable as it allows a quantification of the detected compounds facilitating the determination of the PIONA (paraffins, isoparaffins, olefins, naphthenes, and aromatics) composition.^{18,29,30} These analyses have shown the major differences between plastic pyrolysis oils and conventional crude oil feedstocks as the plastic oils have an increased fraction of (di)olefins and aromatics and span a wider carbon range up to C₈₀. Although GC × GC-FID, especially equipped with reversed phase columns, is highly powerful to characterize complex mixtures, it still struggles with the detailed separation of the complex heavy tail of pyrolysis oils.³⁰ High-magnetic-field ultrahigh-resolution mass spectrometry, known as Fourier transform ion cyclotron resonance mass spectrometry (FT-ICR MS), can complement GC × GC-FID analysis for plastic pyrolysis oils, especially as it can analyze high-molecular-weight compounds,³² assess species with a high heteroatom content,^{33,34} and differentiate between complex unsaturated hydrocarbons.³⁵ In recent years, FT-ICR MS has already been used for the analysis of plastic pyrolysis oils.^{36–44} However, these studies focused on the hydrocarbon content of one mixed plastic waste pyrolysis oil and less on heteroatom-containing components.

Indeed, in addition to hydrocarbons, plastic waste pyrolysis oils typically contain between 1 and 5 wt % of heteroatoms of

which oxygen is the most prevalent.^{18,29,31} During pyrolysis, these heteroatoms partly transfer into the pyrolysis oils. The total amount of heteroatoms (i.e., hydrocarbon, carbon, nitrogen, sulfur, and oxygen) can be tentatively quantified by combustion elemental analysis. However, the detection of oxygen via elemental analysis is challenging as the limit of detection is as high as 1000 ppm for conventional methods. Furthermore, to design upgrading techniques, next to the absolute concentrations of heteroatoms, knowledge of the detailed chemical form in which they are present is also essential. For this purpose, GC \times GC can be employed to identify compounds with specific heteroatoms. By employing GC \times GC-TOF-MS, Toraman et al. characterized 2.3 wt % oxygenated compounds in a plastic pyrolysis oil including components with up to 17 carbon atoms.²⁹ The majority of oxygenates detected were phenols and ketones, especially for smaller oxygenates with less than 8 carbon atoms. Additionally, one-dimensional GC-MS can also be employed to quantify oxygenates present in plastic pyrolysis oils despite being less informative and accurate than two-dimensional comprehensive GC \times GC.³¹ Mass spectrometry without a prior GC separation can further elucidate the composition of oxygenates present in plastic pyrolysis oils. Here, FT-ICR MS has also been used to investigate the molecular structure of oxygenates within pyrolysis oils. Ware et al. investigated the composition of one plastic pyrolysis oil and compared it to a biomass and municipal waste oil.^{38,39} They identified oxygenated hydrocarbons with up to four oxygens and a carbon number of 55 in the plastic pyrolysis oil. Mase et al. employed three different ionization methods to analyze the oxygen content of a mixed plastic waste pyrolysis oil.³⁶ They also predominantly observed aromatics with one to four oxygen atoms. However, no clear contaminant sources have been pinpointed, and only one type of plastic waste pyrolysis oil was studied. This makes it unclear how additives, organic waste, or other trace polymers influence the composition and whether the composition is dependent on the type of polymer.

In this work, the molecular composition of four different plastic pyrolysis oils has been analyzed by ultrahigh-resolution 21 T FT-ICR MS. FT-ICR MS allows the determination of the accurate molecular mass and assigns unique molecular formulas to all ionized species within the pyrolysis oils with a minimum carbon number of 13 and no limitations in the heteroatom content. The four different plastic pyrolysis oils were produced from three postconsumer waste samples consisting of different polyolefins, i.e., PE, PP, and mixed polyolefins (MPO). In addition to the three waste samples, one pyrolysis oil produced from virgin LDPE has been analyzed. Every sample has been analyzed with two different ionization modes: positive-ion atmospheric-pressure photoionization [(+)APPI] and negative electrospray ionization [(-)ESI]. Each of these ionization modes promotes the identification of different molecules present in the pyrolysis oils.⁴⁵ (+)APPI is excellent for the identification of the hydrocarbon matrix, while (-)ESI ionizes mainly oxygenates and acidic contaminants. While, (+)APPI has a lower ionization selectivity for paraffinic species, no other ionization techniques like positive-ion atmospheric-pressure chemical ionization (+)APCI perform better in this regard with postconsumer plastic waste pyrolysis oils.⁴⁴ This is of no concern as the paraffinic content of these pyrolysis oils is well-characterized with GC methods. The combination of these two ionization modes allows to paint a picture of the hydrocarbons

and oxygenates present in the four pyrolysis oils. Due to the ultrahigh resolution of the applied 21T FT-ICR MS, we could identify the molecular composition of the heavy fraction (C₁₃₊) of the pyrolysis oils and its contaminants with an unprecedented level of molecular detail.

2. MATERIALS AND METHODOLOGIES

2.1. Materials. Four different plastic pyrolysis oils were analyzed throughout this work, including three postconsumer plastic pyrolysis oils (PE, PP, and MPO) and one pyrolyzed virgin LDPE sample. The three sorted postconsumer plastic waste pyrolysis oils were produced in earlier work, where more details can be found.¹⁸ In short, the original plastic waste samples were acquired from the recycling company Ecoo (Belgium). The postconsumer PE stems from polymers used in film applications, the PP sample is a mixture of PP from rigid applications, and the MPO also comes from rigid applications. These waste fractions accurately represent the sorted outlet streams of a typical European plastic waste sorting plant, having undergone authentic preprocessing procedures such as shredding, washing, drying, and sorting. Due to imperfect sorting, the investigated polyolefin blends comprise trace amounts of other polymers and (in)organic residues that have accrued during the prior utilization of these plastic materials. The virgin LDPE was a film-grade LDPE LD 150 series grade (Exxonmobil) with a melt flow index of 0.75 (g/10 min at 190 °C/2.16 kg, ASTM D1238) and a density of 923 kg m⁻³ (ASTM D1505).

All plastic blends underwent thermal pyrolysis in a pilot-scale pyrolysis unit. The pyrolysis process involved the utilization of an extruder to introduce postconsumer waste into a heated continuously stirred tank reactor (CSTR). The unit maintained a consistent feeding rate of 1 kg/h, while the CSTR operated at 450 °C and atmospheric pressure. It was confirmed that steady-state conditions were achieved for all obtained pyrolysis oils. Further information regarding the pilot-scale pyrolysis unit can be found in our previous work.¹⁸

The obtained postconsumer plastic pyrolysis oils were characterized by elemental analysis and GC \times GC-FID.¹⁸ The virgin LDPE pyrolysis oil sample was also characterized by GC \times GC-FID at the same conditions. The obtained hydrocarbon composition of the LDPE pyrolysis oil is provided in the [Supporting Information](#). Supplementary analyses using inductively coupled plasma-optical emission spectroscopy (ICP-OES) and combustion ion chromatography (CIC) were conducted to provide additional insights into the elemental composition of the postconsumer plastic pyrolysis oils. The CIC method facilitates the quantification of halogens, whereas ICP-OES specifically targets the elemental metal compositions. As the virgin LDPE contained only pure polymers and a limited share of additives, no ICP-OES or CIC characterization was performed on this sample.

2.2. 21 T FT-ICR MS. Two different ionization modes were employed in this work to analyze the hydrocarbons and oxygenates using a custom-built 21 T FT-ICR mass spectrometer.⁴⁶ (+)APPI offers a high reproducibility and a more uniform ionization response among different species (e.g., hydrocarbons and heteroatom-containing species), reducing the biases toward specific compound families (e.g., carboxylic acids).^{47–49} Therefore, (+)APPI is ideally suited for analyzing the hydrocarbon content in the four different polymer pyrolysis oils. On the other hand, (-)ESI targets the ionization of acidic and oxygenated compounds, making it well-suited for analyzing oxygenates within the four pyrolysis oils.⁴⁵

For (+)APPI, the plastic pyrolysis oils were prepared and ionized as follows. The plastic pyrolysis oils were dissolved in a toluene:methanol solution (1:1 volumetric ratio) at a concentration of 50 μ g/mL prior to injection. Methanol was required to fully dissolve the polar oxygen-containing species within the plastic pyrolysis oils. An Ion Max APPI source from Thermo Fisher Scientific, Inc. (San Jose, CA, USA) was employed with a vaporizer temperature set at 350 °C. Nitrogen (N₂) sheath gas was utilized at 3.44 bar to prevent any contact between the pyrolysis oil and air, and a N₂ auxiliary gas (32 mL min⁻¹) was employed to prevent sample oxidation. Gas-phase

neutrals underwent photoionization through a 10 eV (120 nm) ultraviolet krypton lamp (Syagen Technology, Inc., Tustin, CA, USA). For (−)ESI, the pyrolysis oil samples were also dissolved in 1:1 toluene:methanol at a concentration of 50 μg/mL. Samples were directly infused at 0.55 μL/min and ionized with a needle voltage of −3.2 kV for negative ions.

Ions were analyzed using a custom-built 21 T FT-ICR mass spectrometer.⁴⁶ For the analysis, 2×10^6 charges were accumulated for approximately 1–5 ms in an external multipole ion trap equipped with automatic gain control, or AGC.⁵⁰ Ion depletion, a method for mass filtering or gas-phase depletion of contaminant ions,⁵¹ was employed to enhance the signal-to-noise ratio by dampening the abundance of species with a mass-to-charge ratio (m/z) between 306–334 Da due to an unknown compound in the samples.

Ions were transferred to the ICR cell based on their m/z values, and subsequent excitation to an m/z -dependent radius was performed to optimize the dynamic range and the number of detected peaks. Excitation and detection occurred on the same pair of electrodes of the dynamically harmonized ICR, which operated with a 6 V trapping potential. Time-domain transients of 3.2 s were acquired using Predator software, and 100 time-domain transients were averaged for all samples. Spectra were internally calibrated using an extended homologous alkylation series of high relative abundance before peak detection ($>6\sigma$ baseline root-mean-square (RMS) noise) and automated elemental composition assignment. These homologous alkylation series comprised series of paraffins, olefins, and diolefins (DBE = 0, 1, and 2) to ensure that the entire mass spectrum was covered. PetroOrg software facilitated molecular formula calculation and data visualization in plots of double bond equivalent (DBE) vs carbon number. The DBE is defined by eq 1 and represents the number of double bonds and cyclic rings for hydrocarbons, with C denoting the number of carbon atoms and H the number of hydrogen atoms. The number of oxygen atoms does not influence the DBE.

$$\text{DBE} = C - \frac{H}{2} + 1 \quad (1)$$

Only molecular formulas with an error below ~0.10 ppm were kept for data interpretation, and only compound classes with a relative abundance of $\geq 0.15\%$ and at least three different molecular formulas were considered for data analysis. The latter criterion stems from the fact that it is unlikely that for example only two molecular formulas would be identified for one compound class in a complex mixture as a plastic pyrolysis oil.

3. RESULTS AND DISCUSSION

3.1. Hydrocarbons [(+)APPI]. (+)APPI is known to ionize the hydrocarbon matrix well and has been used to identify the hydrocarbons present in all four pyrolysis oils. Figure 1 displays the plots of the DBE versus carbon number for the hydrocarbons of the four samples. The plastic pyrolysis oils displayed a carbon range from C₁₃ to C₈₂ for the three waste oils, whereas the virgin pyrolysis oil contained species up to C₇₀. The fractions lighter than C₁₃ were not measured by FT-ICR MS but were determined via GC × GC (see the Supporting Information).¹⁸ Note that FT-ICR MS is a semiquantitative method at best, making it unreliable to determine a PIONA composition based on this. Therefore, the supplied GC × GC measurements provide an accurate quantitative detailed PIONA composition of the pyrolysis oils. FT-ICR MS adds another level of detail to the identification of heteroatom-containing species and heavy or polyaromatic hydrocarbons.

A distinction is made between odd-electron ions, corresponding to ionized radicals, and even-electron ions, corresponding to protonated molecules. With (+)APPI, a dominant fraction of odd-electron hydrocarbons is observed, similar to what is found in the literature.³⁶ The radical cations

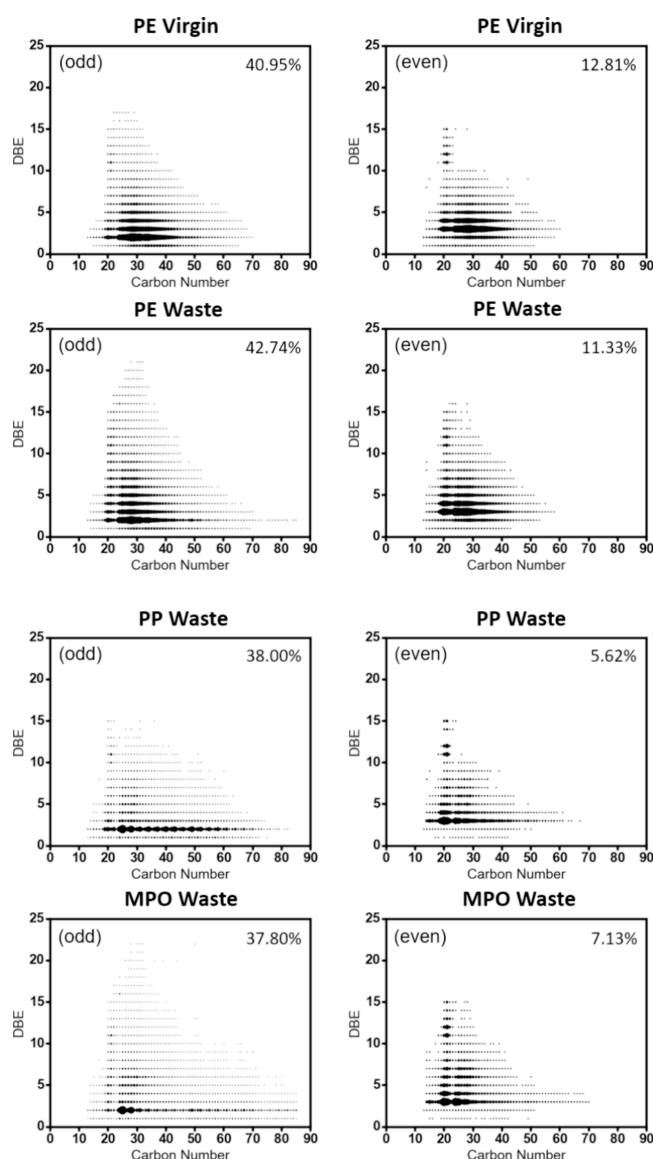


Figure 1. (+)APPI-mode DBE versus carbon number plots for hydrocarbons from the virgin LDPE, PE waste, PP waste, and MPO waste. The area of the dots is proportional to the relative abundance of the respective molecular formula. Odd-electron ions (left) and even-electron ions (right) are presented with the relative abundance of every class presented in the top right corner.

(odd-electron) exhibited a significantly broader variation in both the carbon number and double bond equivalents (DBE) compared to the protonated species. The most prevalent molecular formulas for the odd-electron configuration have a DBE of two, representing diolefins and cyclic olefins. In contrast, for the even-electron ions, the predominant DBE is three, possibly corresponding to triolefins or cyclic diolefins. These observed trends are in agreement with what is observed in the literature.^{36,44} The carbon number distribution of FT-ICR MS corresponds well with the analysis by GC × GC,¹⁸ which quantified hydrocarbons up to C₇₅, proving that with proper GC columns, the latter technique is also suitable for the analysis of very heavy hydrocarbon feedstocks. All samples in Figure 1 contain a dip in signal-to-noise between C₂₁–C₂₄ due to the “ion depletion” or mass filter required to reduce the abundance of prominent contaminant peaks in the pyrolysis

oils and improve the signal-to-noise ratio of the ions of interest. A highly abundant peak at approximately 322 Da within this m/z range can act as a potential contaminant, leading to significant ion suppression.

The monoalkenes and cycloalkanes can be identified at a DBE of 1. At higher DBEs, diolefins (DBE = 2), monoaromatics (DBE = 4), and fused aromatic compounds (DBE \geq 6) are found. The area at a DBE of 10–15 and C_{20} comprises highly unsaturated polynuclear aromatics, known as coke precursors, which are identified in all four samples. For example, $C_{28}H_{14}$ was found in MPO, which is an eight-ring polyaromatic such as for example bisanthene or benzocoronene for which the molecular structures are provided in Figure 2. The exact molecular structures of the identified $C_{28}H_{14}$ cannot be determined by FT-ICR MS.

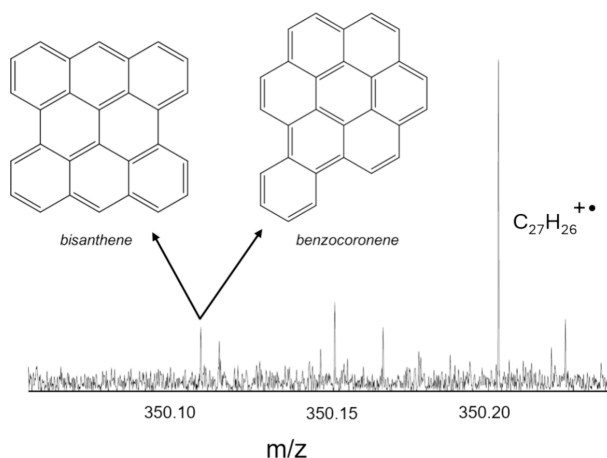


Figure 2. Molecular structures of bisanthene and benzocoronene, which correspond to molecular formulas assigned to mass spectral peaks detected by (+)APPI 21 T FT-ICR MS in MPO pyrolysis oil.

While the area of the dots in Figure 1 is proportional to the relative abundance, it should be noted that the relative abundances of FT-ICR MS are semiquantitative at best. This is due to mass spectrometry detecting ions, and the ionization efficiency or “monomer ion yield” is affected by the molecular structure and even intermolecular interactions or aggregation state of the sample.^{52–54} All samples revealed a decrease in the carbon number range as a function of increasing DBE values. For instance, for the diolefins (DBE = 2), the PE waste pyrolysis oil revealed compounds up to C_{82} ; conversely, species with a DBE of 21 only featured up to C_{32} . This decrease is attributed to the fact that the polyaromatic (high DBE), heavier hydrocarbons remain in the char, a solid that is not the focus of the present study; the work herein presents only the analysis of the liquid pyrolysis oil.

All studied pyrolysis oils consist of a wide range of (un)saturated hydrocarbons as presented in Figure 1. A wide diversity of aromatics was observed for both the virgin and postconsumer PE waste pyrolysis oil. Overall, the FT-ICR MS analyses of virgin LDPE and PE waste pyrolysis oils reveal similar trends for the abundance of hydrocarbons. Nevertheless, the postconsumer waste pyrolysis oil features a more complex collection of polycyclic aromatic hydrocarbons (PAH), particularly with a DBE > 17. The existence of these coke precursors in the PE waste pyrolysis oil demonstrates the higher tendency of waste plastics to form aromatics during pyrolysis compared to the virgin material, which has been

reported in the literature.^{55,56} With FT-ICR MS, it is observed that there is not only more coke formation in postconsumer plastic pyrolysis compared to virgin plastics but that the produced coke contains more aromatic rings. The first reason for the larger occurrence of coke precursors is the presence of ill-sorted polymers in the waste PE fraction. As waste PE mostly stems from polymer film applications, these traces are for example polystyrene (PS), polyethylene terephthalate (PET), or even polyvinyl chloride (PVC), among others, stemming from multilayer packaging.⁵⁷ The presence of styrene and elevated concentrations of chlorine in the waste PE pyrolysis oil confirms the presence of PS and PVC in this sample.¹⁸ The aromatics formed during pyrolysis of those ill-sorted polymers can then undergo alkylation and cyclization reactions to form PAHs, increasing the share of (complex) aromatics in the final product.^{58,59} In addition, polymer additives such as stabilizers or phthalates stemming from the catalyst can also contribute to the aromatic fraction in the waste pyrolysis oils. Furthermore, the waste pyrolysis oil contains metals as demonstrated by ICP-OES analysis.¹⁸ These metals such as Fe, K, and Na are known to act as catalysts for coke formation, thus enhancing the rate of aromatic formation.^{25,60} The last potential reason for the difference in aromatics is the higher fraction of defects and oxygenates caused by aging during the polymer lifecycle. These defects will result in a faster dissociation, higher polymer conversion, and as a result a higher selectivity toward aromatics.⁶¹

Next, a comparison between the three oils of the postconsumer plastic wastes will be made. The waste PE pyrolysis oil contains a higher fraction of aromatic species compared to the waste PP. During thermal pyrolysis, aromatic compounds are typically formed by cyclization reactions between a linear diolefin and olefin such as Diels–Alder reactions or via cyclization reactions of a radical olefin.⁶² In theory, branched (di)olefins also cause cyclization, but the reaction rates are limited due to steric hindrance of the branches. As a result, polypropylene pyrolysis oil contains less cyclic compounds and more diolefins. The higher fraction of aromatics in the postconsumer PE oil can also be attributed to a higher fraction of other polymers such as polystyrene, which decompose to aromatic compounds. Furthermore, it should be noted that PP pyrolysis results in iso-olefins and diolefins, which differ in carbon number by three carbon atoms. This is because PP is rich in tertiary carbon atoms resulting in a more stable tertiary radical intermediate for depolymerization instead of secondary radicals with polyethylene.¹⁰ As a result, an elevated product selectivity toward these iso-olefins and diolefins is found. Hassibi et al. observed a similar PP pyrolysis oil composition with a major fraction of diolefins and the depolymerization products of PP analyzed by atmospheric-pressure chemical ionization (APCI) FT-ICR MS.³⁷

Looking at the DBE vs carbon number plot of the MPO waste pyrolysis oil, its hydrocarbon composition appears to be a mix of both the PE and PP waste pyrolysis oils. For example, both the depolymerization trend of PP, with repeating units of three carbons, and the complex PAHs present in PE are observed. It should, however, be noted that FT-ICR MS is not quantitative as it is limited by selective ionization.⁴⁵ From GC \times GC-FID, it is known that the MPO pyrolysis oil consists of more aromatic species compared to the waste PE and PP pyrolysis oils, indicating that the pyrolyzed MPO fraction is not just a mix of PE and PP but also contains a higher amount of ill-sorted polymers causing a higher aromatic content in the

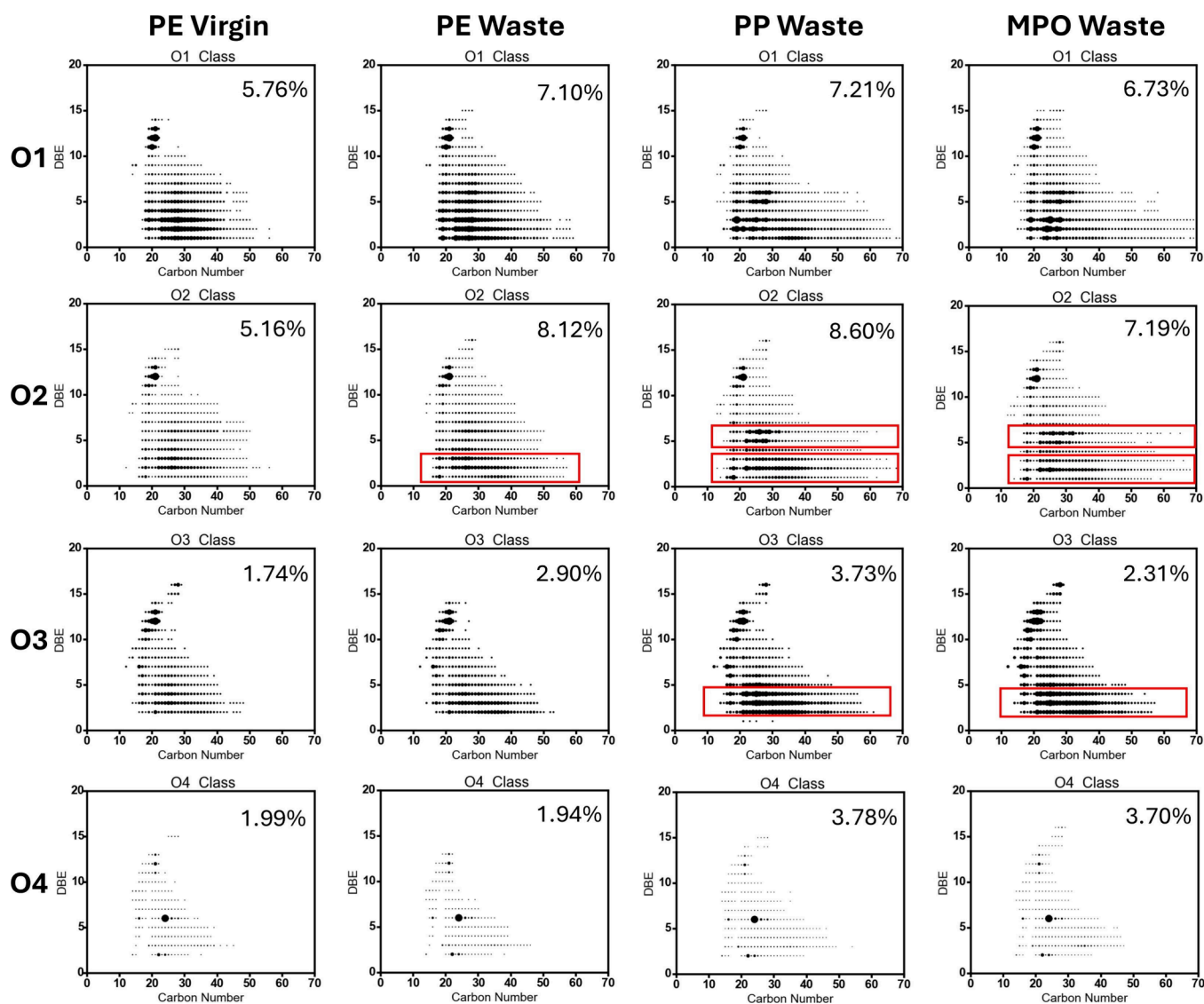


Figure 3. (+)APPI-mode DBE versus carbon number for oxygenates from the virgin LDPE, PE waste, PP waste, and MPO waste with relative abundances per molecular class. The area of the dots is proportional to the relative abundance of the respective molecular formula. The mass fraction of oxygen detected by elemental analysis is depicted on top. The major differences between the waste and virgin pyrolysis oils are highlighted in red.

corresponding pyrolysis oil.^{15,63} The presence of PS in the MPO fraction was confirmed by the detection of styrene in the pyrolysis oil by comprehensive two-dimensional GC, which is a product not formed by the pyrolysis of PE or PP but solely by PS pyrolysis.⁶⁴ The aromatics formed during the pyrolysis of PS and PET will thus increase the fraction of aromatics produced by PE and PP even further, resulting in the high aromatic content of MPO. Furthermore, Klaimy et al. reported that the thermal pyrolysis of PE and PP mixtures resulted in a higher aromatics content than the separate pyrolysis of PP and PE.⁶³

3.2. Oxygen. Oxygen is one of the most abundant heteroatoms present in plastic pyrolysis oils. The presence of oxygen in virgin polymers stems from polymer additives such as antioxidants, stabilizers, plasticizers, etc.^{65–68} For plastic waste, the oxygen content can be attributed to ill-sorting of other polymers such as PET, acrylates, or ethylene-vinyl acetate (EVA) and to organic residues accumulated during usage of the plastics. During pyrolysis, the majority of the

oxygen is converted into water, carbon dioxide, and carbon monoxide. Oxygen is undesired in plastic waste pyrolysis oils and plastic waste itself as it results in direct CO₂ emissions and thus carbon leakage, i.e., lowering the carbon efficiency of the chemical recycling and hampering application of pyrolysis oils in further (petro-)chemical processes. The results for the characterization of oxygenates accessed via two ionization modes (+)APPI and (–)ESI are discussed in the following sections.

3.2.1. (+)APPI. The (+)APPI targets the ionization of hydrocarbons as discussed previously; however, it can also access heteroatom-containing compounds. Figure 3 presents the DBE versus carbon number plots for four oxygenated classes O1, O2, O3, and O4. The terms O1, O2, O3, and O4 refer to molecules containing respectively one, two, three, and four oxygen atoms in addition to hydrogen and carbon. Every plot displays the relative abundances of the molecular class with respect to the total abundance detected in the sample. No distinction is made between odd- and even-electron ions as the

fraction of odd-electron oxygenates amount to less than 20% for all pyrolysis oils. Moreover, the patterns of odd- and even-electron oxygenates are similar, and therefore, no distinction is made between those. For example, in virgin pyrolysis oil, 5.76% of the relative abundance stems from O1 compounds, O2 molecules are 5.16%, O3 compounds comprise 1.74% of the abundance, and O4 compounds correspond to 1.99% of the abundance. The other detected compounds in addition to O1–O4 for (+)APPI are hydrocarbons and higher-order oxygenates that will be discussed later. Hence, the depicted relative abundance allows us to compare the prevalence of oxygenates within one type of pyrolysis oil. In addition to the relative abundances depicted in Figure 3, hydrocarbons and higher-order oxygenates were detected as will be discussed further. Only for the PE waste pyrolysis oil, a significant fraction of 2100 ppm of oxygenates could be detected by elemental analysis, whereas for the other samples, the amount of oxygen was below the limit of detection of 1000 ppm.

The relative abundance of all waste samples features a similar ratio between O1/O2 and O2/O3. For the virgin LDPE, more O1 oxygenates are detected compared to O2 compounds, indicating a contrast to the waste samples, a topic that will be elaborated on later.

The DBE versus carbon number plots for oxygenates have a similar profile compared to those for hydrocarbons. The plastic pyrolysis oils show a wide variety of oxygenated molecules in the waste and virgin pyrolysis oil. Moreover, there is a considerable similarity in the molecules detected between the waste and virgin pyrolysis oils. These two observations suggest that the oxygenated compounds detected are reaction products formed during thermal pyrolysis and that there are few unconverted oxygen-containing impurities detected by (+)APPI. During thermal pyrolysis, the majority of oxygen is converted to carbon dioxide and carbon monoxide. This was also found by elemental analysis of the oxygen content of solid PE waste compared to the corresponding pyrolysis oil. The oxygen content of the solid waste was eight times higher than that of the pyrolysis oil, indicating that most oxygen was converted into carbon oxides and water.¹⁸ However, the formed carbon dioxide and especially the highly reactive carbon monoxide can react with the hydrocarbon matrix and form the oxygenates detected by (+)APPI. Another potential pathway is the reaction of released hydroxyl radicals with the hydrocarbon matrix.

It is observed in Figure 3 that the lower limit of the DBE for O1 and O2 species is one, while for O3 and O4, this lower limit was two. As the presence of a carbonyl group will increase the DBE by a value of one, this lower limit makes the O3 and O4 species contain at least two carbonyl groups. The fact that the lower limit of the DBE correlates with the amount of oxygen makes it unlikely in the case of O3 and O4 that the presence of olefins determines the increase in DBE.

For all oxygenated classes, highly aromatic compounds (DBE ≥ 5) reveal higher abundances compared to the aromatic species detected in hydrocarbons. This shows a clear preference of carbon oxides to react with aromatic hydrocarbons compared to aliphatic compounds. A typical reaction between carbon monoxide and the hydrocarbon matrix is the addition reaction of the carbon monoxide to a radical hydrocarbon with the formation of an aldehyde compound. The carbon monoxide insertion (carbonylation) can be catalyzed by metals such as Ni or Co, which are present in the plastic pyrolysis oil.^{69–71} The bond dissociation energy of

the carbon–carbon bond of ethanal and benzaldehyde is illustrated in Figure 4.^{72,73}

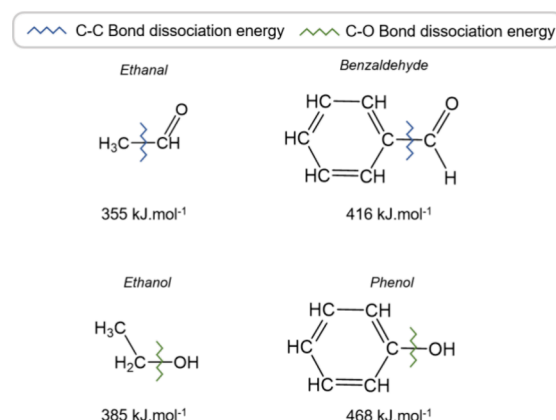


Figure 4. Bond dissociation energies of the C–C bond of ethanal and benzaldehyde and the C–O bond of ethanol and phenol. Data obtained from references.^{72,73}

The bond dissociation energy of the C–C bond in the aliphatic ethanal is 61 kJ mol^{-1} lower compared to that of the aromatic benzaldehyde C–C bond. This will result in a significantly lower reaction enthalpy and therefore higher thermodynamic driving force for carbon monoxide addition to aromatic compounds. A similar reasoning holds for alcohols, which are formed by reduction of aldehydes and the reaction of hydroxyl radicals with the hydrocarbon matrix. The C–O bond dissociation energy of ethanol is 83 kJ mol^{-1} lower than the corresponding phenol bond (see Figure 4). Therefore, the superior stability of phenolic compounds will contribute to more aromatic oxygenates than aliphatic ones.

Data derived from (+)APPI highlight the preferential occurrence of secondary reactions that produce oxygen-containing compounds with high DBE values. As observed in Figure 3, mainly at a DBE between 11 and 13 and a carbon number of 19–22, a prominent mass spectral peak for oxygenates is observed for O1, O2, and O3. These are undoubtedly polyaromatic structures, which can correspond to a wide variety of possible structures among which the most thermodynamically stable consists of three aromatic rings. Some potential molecular structures are provided in the Supporting Information (Figure S1). These reaction products highlight the preference for secondary reactions between carbon oxides and hydroxyl radicals with aromatic hydrocarbons. Similarly for the hydrocarbons, an elevated abundance of compounds at DBE of 11–13 and with a carbon number of 21 is found in all samples (see Figure 1), indicating that the deoxygenation of these compounds occurs. As the prominence of the oxygenates at this DBE and carbon number is much more profound than the corresponding hydrocarbons, this supports the claim that the hydrocarbons stem from deoxygenation reactions of structures as depicted in Figure S1.

Next to the discussed O1–O3 oxygenates in Figure 3, compounds up to O7 have been detected in MPO pyrolysis oil. Figure 5 depicts the relative abundances of the oxygenates detected by (+)APPI for the four pyrolysis oils. Similar to what is found in the literature, most oxygenates contain one to four oxygen atoms.^{36,38,39} The O5–O7 classes are a minor component of all samples with a relative abundance lower than 0.6 wt %, while most oxygen-containing compounds

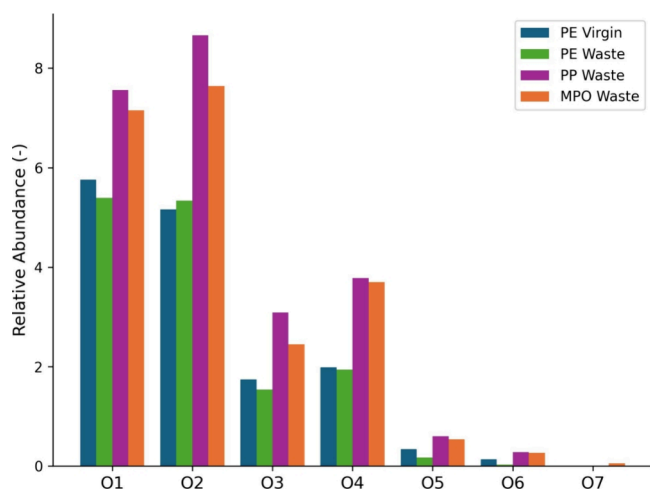


Figure 5. Class distributions of relative abundance of the oxygenates detected by (+)APPI for virgin LDPE pyrolysis oil, PE waste pyrolysis oil, PP waste pyrolysis oil, and MPO waste pyrolysis oil.

contain one or two oxygen atoms. The relative abundance of the O4 class is comparable to the class of O3. Figure 6 displays

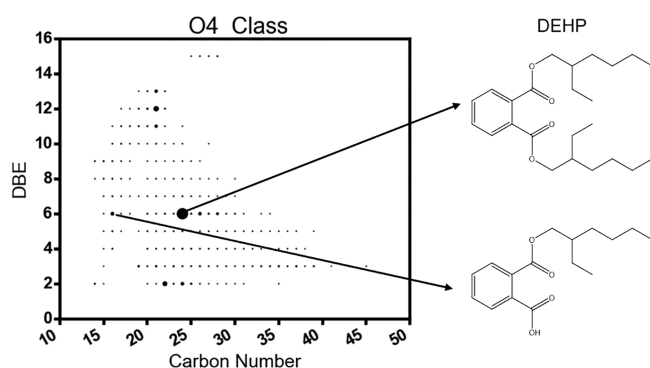


Figure 6. DBE versus carbon number plot of even-ion O4 for waste PP pyrolysis oil by (+)APPI with (top) diethylhexyl phthalate (DEHP) and (bottom) 2-(((2-ethylhexyl)oxy)carbonyl)benzoic acid indicated.

the DBE versus carbon number plot of O4 for the waste PP pyrolysis oil. The O4 composition of the waste PP pyrolysis oil is comparable to the other postconsumer waste pyrolysis oils. The distribution of O4 molecules is markedly different from the O1–O3 plots. In contrast to the O1–O3 distribution, there is a high relative abundance of species in a limited number of molecules instead of a wide distribution.

It has to be noted that FT-ICR MS does not allow the identification of the detailed molecular structure. Therefore, a combination of sample knowledge and experimental data is required to hypothesize the molecular structure of the abundantly detected $C_{24}H_{38}O_4$. It is expected that diethylhexyl phthalate (DEHP) corresponds to the detected $C_{24}H_{38}O_4$, which is a common internal donor in catalysts to control the isotacticity of PP.⁷⁴ DEHP is detected in all three analyzed pyrolysis oils, as all oils contain a fraction of PP. This is also confirmed by the lower abundance of O4 found in the waste PE oil compared to the waste MPO and PP samples. During thermal pyrolysis, DEHP breaks down due to the scission of the C–O ester bond with formation of 2-(((2-ethylhexyl)oxy)carbonyl)benzoic acid and 3-methyleneheptane. The

reaction product, 2-(((2-ethylhexyl)oxy)carbonyl)benzoic acid, is also detected by (+)APPI. Next to breaking the C–O ester bond, a decarboxylation is expected with formation of benzene and carbon dioxide. The correlation between the share of PP in the plastic waste and the amount of $C_{24}H_{38}O_4$ detected, combined with its use as a catalyst donor and the identification of the most likely thermal dissociation product of DEHP, makes it highly likely that DEHP effectively corresponds to the observed $C_{24}H_{38}O_4$. The example above illustrates how plastic additives influence the composition of plastic pyrolysis oils and that not all additives break down entirely during thermal pyrolysis. In the following subsection, results from (–)ESI ionization mode will be discussed to further elaborate on the breakdown of oxygen-containing additives and contaminants.

3.2.2. (–)ESI. The (–)ESI mode is very effective at ionizing oxygen-containing molecules. To illustrate this, Figure 7 depicts the DBE versus carbon number plots for four oxygenated classes O1, O2, O3, and O4. With (–)ESI, only even-electron ions are observed. The comparison between the plots of (+)APPI (Figure 3) and (–)ESI (Figure 7) reveals significant differences in terms of the carbon number range at all given DBE values. While with (+)APPI, a wide variety of molecules with similar concentrations were observed, in (–)ESI, a few specific molecules with high concentrations were observed in O1–O4 for all pyrolysis oils. These highly abundant peaks (bold data points in the DBE vs carbon number plots of Figure 7) stem from the thermal dissociation products of specific additives and impurities. The rest of the distribution of molecules, featuring a wide DBE and carbon number range, are reaction products that stem from secondary reactions between carbon monoxides and other oxygenates.

Unlike the (+)APPI measurements, the trends in the relative abundance of the three oxygenated classes differ for the four plastics. The virgin polymer contains relatively more O3 and O4 compounds compared to the postconsumer waste samples, suggesting that the contamination from organic residues and ill-sorted polymers mainly causes an increase in O1 and O2 species. From the elemental analysis, it is known that the MPO and PE waste samples contain the most oxygenates, which corresponds to more O1 oxygenates and less O3 oxygenates compared to the postconsumer PP. The higher oxygen fraction in MPO and PE stems from accumulated oxygenates during the use of these plastics and oxygen-containing additives. The postconsumer PE, which has been collected, comes from plastics used for film applications. These plastics are often multilayer packages where PE is layered with ethylene-vinyl alcohol (EVOH) for barrier properties.^{75–77} Hence, this results in the remaining fraction of EVOH in the PE waste and increases the oxygen fraction in this blend. Moreover, antioxidants are often added to these polymers to ensure the polymer stability during usage. These antioxidants often comprise oxygen-containing groups, producing a higher oxygen share in the corresponding pyrolysis oils.⁶⁸ Lastly, these polymer films are employed in the food industry where organic residues will contaminate the plastic.

In O1, three clear molecule types can be distinguished for all four pyrolysis oils proving that the observed molecules stem from plastic additives and not from the usage of the plastics or other contaminants.^{65,66} The peak at a DBE of 4 consists of both $C_{14}H_{22}O$ and $C_{15}H_{24}O$. While FT-ICR MS does not allow to further elucidate the molecular structure, knowledge about the source of the polymers allows pinpointing the most

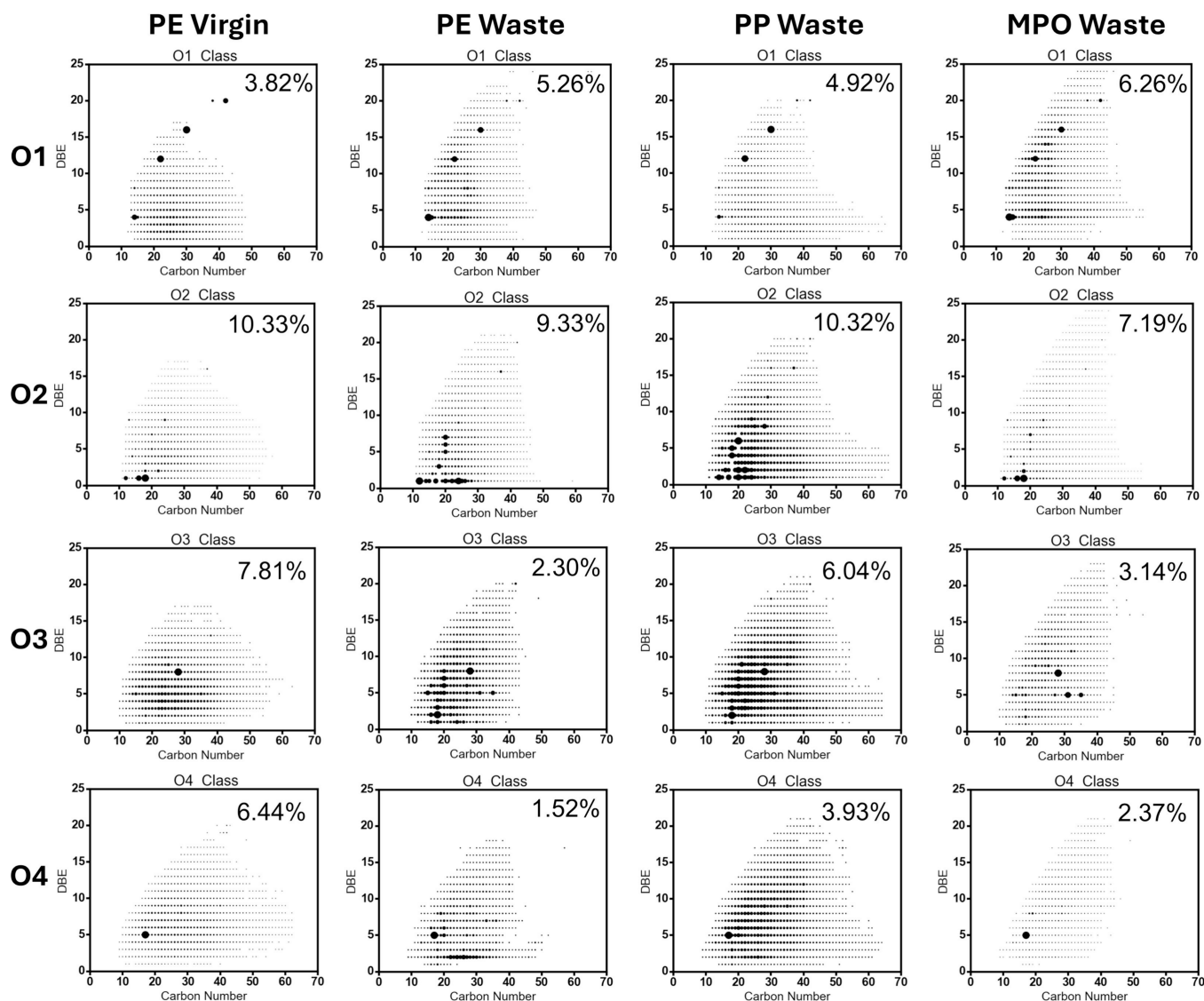


Figure 7. (–)ESI mode DBE versus carbon number for oxygenates from the virgin LDPE, PE waste, PP waste, and MPO waste with relative abundances per molecular class. The area of the dots is proportional to the relative abundance of the respective molecular formula. The mass fraction of oxygen detected by elemental analysis is depicted on top.

likely structure for a given detected molecular formula. For example, 2,6-di-*tert*-butylphenol is a substructure common in antioxidants within polymers such as the common Irganox 1010^{65,66} (see Figure 8). These antioxidants are added with the primary objective that they would react with the remaining radicals present in the polymer, to prevent any thermo-oxidative degradation during the polymer lifetime. Thermal pyrolysis is a radical reaction resulting in the consumption of these antioxidants. During thermal pyrolysis, Irganox 1010 is broken down with formation of 2,6-di-*tert*-butylphenol. No remaining Irganox 1010 was detected in any of the pyrolysis oils, showing full conversion at the applied pyrolysis conditions. Butylated hydroxytoluene (BHT) is another antioxidant that is commonly used within plastics, which was observed via (–)ESI.

Next to the three prominent peaks on the O1 plots, a distribution of other molecules is detected for these oxygenates. For clarity, the plots with the peaks for C₁₄H₂₂O, C₁₅H₂₄O, C₂₂H₂₂O, and C₃₀H₃₀O removed are added to the Supporting Information, Figure S2. These graphs again

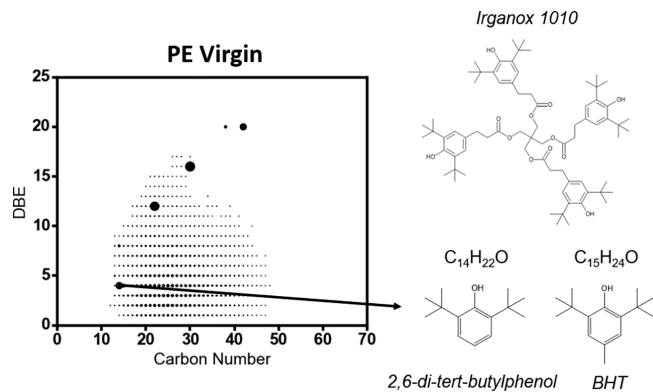


Figure 8. Molecular structures of 2,6-di-*tert*-butylphenol, butylated hydroxytoluene (BHT), and Irganox 1010.

highlight the resemblance of the oxygenates found in the MPO and PE waste. These are molecules formed by secondary reactions between oxygenates and the hydrocarbon matrix. A more distinct area of these molecules is observed for the waste

pyrolysis oils of the PE and MPO compared to the virgin and PP pyrolysis oils. More aromatic oxygenates are formed, especially for the PE and MPO pyrolysis oils, indicating the preference for oxygenated compounds reacting with aromatic species. As the thermal pyrolysis of PE and MPO results in a higher formation of aromatics, the oxygenates are more likely to react, resulting in more O1 oxygenates in PE and MPO than in PP.

The composition of O2 oxygenates differs majorly between the postconsumer waste and the virgin LDPE. Virgin LDPE consists of a wide range of O2 oxygenates with similar relative abundances, while the postconsumer waste has specific molecules with elevated concentrations. Several peaks can be observed for all waste samples, especially at low DBEs. These compounds are likely to be fatty acids such as stearic acid, palmitic acid, and lauric acid, which originate from food remains, cosmetics, and detergents. As these fatty acids are less observed within virgin pyrolysis oil, it is clear that these species stem from the usage of plastic products. During thermal pyrolysis, these carboxylic acids are converted into linear hydrocarbons and carbon dioxide, but these are clearly not fully converted with the currently applied process conditions. The fatty acids are higher in concentration for the pyrolysis oil with the highest oxygen content, i.e., the PE waste pyrolysis oil. This indicates that the elevated oxygen content within the PE waste is caused by an increased contamination from these fatty acids, which is logical due to the main use of film packaging in food contact applications.

As previously discussed, O3 oxygenates are relatively less abundant in the postconsumer waste samples compared to the virgin LDPE. This indicates that the thermally pyrolyzed organic residues mostly end up in less complex O1 (by secondary reactions) or in O2 components. The more complex O3 compounds display a few clear peaks of high-concentration compounds. Particularly, $C_{28}H_{42}O_3$ is present in all four pyrolysis oils making it likely that it stems from plastic additives.

Lastly, the O4 oxygenates display a similar pattern across all four pyrolysis oils with a high abundance of $C_{17}H_{26}O_4$ and a wide range of less abundant hydrocarbons. The presence of $C_{17}H_{26}O_4$ in the virgin PE pyrolysis oil proves that this compound stems from a polymer additive. It is highly likely that this structure is a phthalic acid, which was also identified with (+)APPI as shown in Figure 6.

When looking at (+)APPI, there is a remarkable similarity in the molecular composition of the oxygenates between the virgin pyrolysis oil and the three postconsumer waste oils. This similarity across the four pyrolysis oils has also been observed for (−)ESI. It is remarkable that the dominant O1 compounds in all pyrolysis oils stem from plastic additives breaking down and undergoing secondary reactions with the hydrocarbon matrix. This shows for the first time that polymer additives play an essential role in the pyrolysis process and are detrimental to the quality of the obtained pyrolysis oils. Therefore, the design-to-recycle of polymer additives is an essential step toward plastic pyrolysis oils, which are processable in the chemical industry. It was observed that phenol groups and aromatic carboxyl acids are stable oxygenated compounds that are difficult to break down upon thermal pyrolysis. For example, with Irganox 1010, only the 2,6-di-*tert*-butylphenol group was found, while the carboxyl functionality was entirely removed. Consequently, from a recycling perspective, additives with these thermally stable functionalities should be limited in the

plastics or removed prior to thermal pyrolysis, which is not straightforward at present. Next to this, a lot of oxygenates stemming from additives, other polymers, and organic waste break down during thermal pyrolysis and react with the hydrocarbon matrix. The reaction products mainly depend on the number of aromatics formed during thermal pyrolysis. This is one of the two distinct differences observed between the four organic mixtures. Within PE and MPO, more O1 oxygenates are observed, as these plastics cause the formation of more aromatics resulting in an elevated contribution of secondary reactions. Subsequently, a larger fraction of fatty acids has been observed for the postconsumer waste compared to the virgin LDPE pyrolysis oil. Therefore, decontamination strategies of plastic waste should focus on these compounds to facilitate an improved chemical recycling.

4. CONCLUSIONS

An extensive FT-ICR MS characterization of postconsumer PE, PP, and MPO pyrolysis oils and virgin LDPE pyrolysis oil was conducted, employing both (+)APPI and (−)ESI to analyze the hydrocarbon and oxygen content. The presence of aromatic polymers such as PS and PET, an increased metal content, and the presence of polymer defects in postconsumer PE clearly affected the hydrocarbon composition and the formation rates of aromatics upon thermal pyrolysis. Consequently, the postconsumer PE pyrolysis oil had a higher fraction of aromatics and PAH than the virgin LDPE pyrolysis oil. Furthermore, a considerable resemblance was found when comparing the composition of the MPO with the PE and PP waste. Even though it is known that interactions between the PE and PP in MPO occur upon thermal pyrolysis, no distinct compounds differing from both PE and PP were observed in MPO pyrolysis oil.

The analysis of the oxygenates for the four plastic pyrolysis oils displayed a remarkable similarity between the four analyzed pyrolysis oils, especially with (+)APPI. This resemblance indicates how most oxygenates present dissociate, after which a fraction reacts with the hydrocarbon matrix. The oxygenated compounds detected by (+)APPI show a tendency to react with aromatic compounds over aliphatic structures because of the higher stability of the formed aromatic oxygenates. This makes the removal of oxygen-containing compounds even more important for polymers where thermal pyrolysis results in a high fraction of aromatics as a higher fraction of oxygen will have reacted with the hydrocarbon matrix. Moreover, the produced aromatic oxygenates are more difficult to hydrogenate than aliphatic oxygenates. Hence, the removal of oxygenates is essential for polystyrene, MPO, and PE waste, while PP forms less aromatics resulting in less (aromatic) oxygenates in PP oils. When one wants to limit the oxygen content in polymer pyrolysis oils, it is therefore not only critical to limit the presence of oxygen-containing polymers, additives, and organic residue but also focus on limiting the presence of aromatic products by reducing aromatic polymers and the metal content. The latter will reduce the aromatic fraction formed during pyrolysis, as metals catalyze aromatic formation, resulting in less aromatic hydrocarbons reacting with oxygen.

With (−)ESI, certain contaminants and their reaction products could be pinpointed. All samples (including the virgin LDPE) contained remains of antioxidants (Irganox 1010 and BHT). However, (−)ESI showed a clear difference between the postconsumer waste and the virgin samples. In

the waste pyrolysis oils, fatty acids (from food and detergents) and more complex oxygenated aromatics were observed. These results show that not all oxygenates fully break down upon thermal dissociation at these process conditions.

This study provides fundamental insights into the chemistry of oxygenated contaminants in plastic pyrolysis oils, aiding in the development of improved decontamination strategies. These strategies may include enhanced removal of metals and trace polymers and solvent extraction to remove the aromatic fraction, thus reducing the oxygen content of the pyrolysis oils. Such improvements will make plastic pyrolysis oils more suitable for further chemical processing, closing the loop for polyolefin waste.

■ ASSOCIATED CONTENT

SI Supporting Information

The Supporting Information is available free of charge at <https://pubs.acs.org/doi/10.1021/acs.energyfuels.4c03835>.

(S1) GC × GC-FID results of virgin LDPE pyrolysis oil; (S2) illustration of abundant oxygenate molecular structures detected by (+)APPI; (S3) (−)ESI results of O1 compounds filtered for C₁₄H₂₂O, C₁₅H₂₄O, C₂₂H₂₂O, and C₃₀H₃₀O (PDF)

■ AUTHOR INFORMATION

Corresponding Author

Kevin M. Van Geem – Laboratory for Chemical Technology, Department of Materials, Textiles and Chemical Engineering, Ghent University, Ghent 9052, Belgium; orcid.org/0000-0003-4191-4960; Email: Kevin.VanGeem@UGent.be

Authors

Yannick Ureel – Laboratory for Chemical Technology, Department of Materials, Textiles and Chemical Engineering, Ghent University, Ghent 9052, Belgium; orcid.org/0000-0001-6883-320X

Martha L. Chacón-Patiño – Ion Cyclotron Resonance Program, National High Magnetic Field Laboratory, Florida State University, Tallahassee, Florida 32310, United States; International Joint Laboratory for Complex Matrices Molecular Characterization, iC2MC, TRTG, Harfleur 76700, France; orcid.org/0000-0002-7273-5343

Marvin Kusenberg – Laboratory for Chemical Technology, Department of Materials, Textiles and Chemical Engineering, Ghent University, Ghent 9052, Belgium; orcid.org/0000-0002-3733-3293

Anton Ginzburg – Department of Chemical Engineering, KU Leuven, Diepenbeek 3590, Belgium; orcid.org/0000-0001-7022-7014

Ryan P. Rodgers – Ion Cyclotron Resonance Program, National High Magnetic Field Laboratory, Florida State University, Tallahassee, Florida 32310, United States; International Joint Laboratory for Complex Matrices Molecular Characterization, iC2MC, TRTG, Harfleur 76700, France; Department of Chemistry and Biochemistry, Florida State University, Tallahassee, Florida 32308, United States; orcid.org/0000-0003-1302-2850

Maarten K. Sabbe – Laboratory for Chemical Technology, Department of Materials, Textiles and Chemical Engineering, Ghent University, Ghent 9052, Belgium; orcid.org/0000-0003-4824-2407

Complete contact information is available at:

<https://pubs.acs.org/10.1021/acs.energyfuels.4c03835>

Notes

The authors declare no competing financial interest.

■ ACKNOWLEDGMENTS

Yannick Ureel acknowledges financial support from the Fund for Scientific Research Flanders (FWO Flanders) through the doctoral fellowship grant 1185822N. A portion of this work was performed at the National High Magnetic Field Laboratory, which is supported by the National Science Foundation Division of Materials Research and Division of Chemistry through DMR-2128556 and the State of Florida. The authors acknowledge financial support by the Catalisti-ICON project (HBC.2018.0262) MATTER (Mechanical and Thermochemical Recycling of mixed plastic waste) funded by Flanders Innovation & Entrepreneurship (VLAIO). The authors acknowledge funding from the European Research Council under the European Union's Horizon 2020 research and innovation program/ERC grant agreement no. 818607.

■ REFERENCES

- (1) Lange, J.-P. Towards circular carbo-chemicals – the metamorphosis of petrochemicals. *Energy Environ. Sci.* **2021**, *14* (8), 4358–4376.
- (2) IEA *The Future of Petrochemicals*; IEA: Paris, 2018. <https://www.iea.org/reports/the-future-of-petrochemicals>.
- (3) Ragaert, K.; Delva, L.; Van Geem, K. Mechanical and chemical recycling of solid plastic waste. *Waste Management, Elsevier Ltd* **2017**, *69*, 24–58.
- (4) Francis, R. *Recycling of polymers: methods, characterization and applications*; John Wiley & Sons: 2016.
- (5) *Plastic waste by end-of-life fate - projections*; <https://www.oecd-ilibrary.org/content/data/3f85b1c2-en>.
- (6) Dogu, O.; Pelucchi, M.; Van de Vijver, R.; Van Steenberge, P. H. M.; D'Hooge, D. R.; Cuoci, A.; Mehl, M.; Frassoldati, A.; Faravelli, T.; Van Geem, K. M. The chemistry of chemical recycling of solid plastic waste via pyrolysis and gasification: State-of-the-art, challenges, and future directions. *In Progress in Energy and Combustion Science, Elsevier Ltd* **2021**, *84*, 100901–100901.
- (7) Ignatyev, I. A.; Thielemans, W.; Vander Beke, B. Recycling of polymers: a review. *ChemSusChem* **2014**, *7* (6), 1579–1593.
- (8) Merrington, A. Recycling of plastics. *In Applied plastics engineering handbook*; Elsevier: 2017, pp 167–189.
- (9) *Documentation for greenhouse gas emission and energy factors used in the waste reduction model (WARM)*; U.S. Environmental Protection Agency - Office of Resource Conservation and Recovery: 2016.
- (10) Abbas-Abadi, M. S.; Ureel, Y.; Eschenbacher, A.; Vermeire, F. H.; Varghese, R. J.; Oenema, J.; Stefanidis, G. D.; Van Geem, K. M. Challenges and opportunities of light olefin production via thermal and catalytic pyrolysis of end-of-life polyolefins: Towards full recyclability. *Prog. Energy Combust. Sci.* **2023**, *96*, No. 101046.
- (11) Jung, S.-H.; Cho, M.-H.; Kang, B.-S.; Kim, J.-S. Pyrolysis of a fraction of waste polypropylene and polyethylene for the recovery of BTX aromatics using a fluidized bed reactor. *Fuel Process. Technol.* **2010**, *91* (3), 277–284.
- (12) Encinar, J. M.; González, J. F. Pyrolysis of synthetic polymers and plastic wastes. *Kinetic study. Fuel Processing Technology* **2008**, *89* (7), 678–686.
- (13) Kusenberg, M.; Eschenbacher, A.; Djokic, M. R.; Zayoud, A.; Ragaert, K.; De Meester, S.; Van Geem, K. M. Opportunities and challenges for the application of post-consumer plastic waste pyrolysis oils as steam cracker feedstocks: To decontaminate or not to decontaminate? *Waste Management* **2022**, *138*, 83–115.
- (14) Kusenberg, M.; Roosen, M.; Doktor, A.; Casado, L.; Abdulrahman, A. J.; Parvizi, B.; Eschenbacher, A.; Biadi, E.; Laudou, N.; Jänsch, D.; De Meester, S.; Van Geem, K. M.

Contaminant removal from plastic waste pyrolysis oil via depth filtration and the impact on chemical recycling: A simple solution with significant impact. *Chem. Eng. J.* **2023**, *473*, No. 145259.

(15) Kusenberg, M.; Roosen, M.; Zayoud, A.; Djokic, M. R.; Thi, H. D.; De Meester, S.; Ragaert, K.; Kresovic, U.; Van Geem, K. M. Assessing the feasibility of chemical recycling via steam cracking of untreated plastic waste pyrolysis oils: Feedstock impurities, product yields and coke formation. *Waste Manage.* **2022**, *141*, 104–114.

(16) Orozco, S.; Artetxe, M.; Lopez, G.; Suarez, M.; Bilbao, J.; Olazar, M. Conversion of HDPE into Value Products by Fast Pyrolysis Using FCC Spent Catalysts in a Fountain Confined Conical Spouted Bed Reactor. *ChemSusChem* **2021**, *14* (19), 4291–4300.

(17) Eschenbacher, A.; Varghese, R. J.; Delikonstantis, E.; Mynko, O.; Goodarzi, F.; Enemark-Rasmussen, K.; Oenema, J.; Abbas-Abadi, M. S.; Stefanidis, G. D.; Van Geem, K. M. Highly selective conversion of mixed polyolefins to valuable base chemicals using phosphorus-modified and steam-treated mesoporous HZSM-5 zeolite with minimal carbon footprint. *Applied Catalysis B: Environmental* **2022**, *309*, No. 121251.

(18) Kusenberg, M.; Zayoud, A.; Roosen, M.; Thi, H. D.; Abbas-Abadi, M. S.; Eschenbacher, A.; Kresovic, U.; De Meester, S.; Van Geem, K. M. A comprehensive experimental investigation of plastic waste pyrolysis oil quality and its dependence on the plastic waste composition. *Fuel Process. Technol.* **2022**, *227*, No. 107090.

(19) Zhang, Y.; Ji, G.; Chen, C.; Wang, Y.; Wang, W.; Li, A. Liquid oils produced from pyrolysis of plastic wastes with heat carrier in rotary kiln. *Fuel Process. Technol.* **2020**, *206*, No. 106455.

(20) Kusenberg, M.; Eschenbacher, A.; Delva, L.; De Meester, S.; Delikonstantis, E.; Stefanidis, G. D.; Ragaert, K.; Van Geem, K. M. Towards high-quality petrochemical feedstocks from mixed plastic packaging waste via advanced recycling: The past, present and future. *Fuel Process. Technol.* **2022**, *238*, No. 107474.

(21) Caeiro, G.; Lopes, J. M.; Magnoux, P.; Ayrault, P.; Ramôa Ribeiro, F. A FT-IR study of deactivation phenomena during methylcyclohexane transformation on H-USY zeolites: Nitrogen poisoning, coke formation, and acidity–activity correlations. *J. Catal.* **2007**, *249* (2), 234–243.

(22) Hegedus, L. L.; McCabe, R. W. Catalyst poisoning. In *Studies in Surface Science and Catalysis*; Elsevier: 1980, Vol. 6, pp 471–505.

(23) Marturano, V.; Cerruti, P.; Ambrogi, V. Polymer additives. *Phys. Sci. Rev.* **2017**, *2* (6), No. 20160130.

(24) Amghizar, L.; Dedeyne, J. N.; Brown, D. J.; Marin, G. B.; Van Geem, K. M. Sustainable innovations in steam cracking: CO₂ neutral olefin production. *Reaction Chemistry & Engineering* **2020**, *5* (2), 239–257.

(25) Sundaram, K. M.; Stancato, B. How Much Is Too Much? Feed Contaminants and Their Consequences. In *2018 Spring Meeting and 14th Global Congress on Process Safety*; AIChE: 2018.

(26) Serranti, S.; Bonifazi, G. 2 - Techniques for separation of plastic wastes. In *Use of Recycled Plastics in Eco-efficient Concrete*; Pacheco-Torgal, F., Khatib, J., Colangelo, F., Tuladhar, R., Eds.; Woodhead Publishing: 2019; pp 9–37.

(27) Ruj, B.; Pandey, V.; Jash, P.; Srivastava, V. K. Sorting of plastic waste for effective recycling. *Int. J. Appl. Sci. Eng. Res.* **2015**, *4* (4), 564–571.

(28) Kusenberg, M.; Roosen, M.; Doktor, A.; Casado, L.; Jamil Abdulrahman, A.; Parvizi, B.; Eschenbacher, A.; Biadi, E.; Laudou, N.; Jansch, D.; et al. Contaminant removal from plastic waste pyrolysis oil via depth filtration and the impact on chemical recycling: A simple solution with significant impact. *Chemical Engineering Journal* **2023**, *473*, No. 145259.

(29) Toraman, H. E.; Dijkman, T.; Djokic, M. R.; Van Geem, K. M.; Marin, G. B. Detailed compositional characterization of plastic waste pyrolysis oil by comprehensive two-dimensional gas-chromatography coupled to multiple detectors. *Journal of Chromatography A* **2014**, *1359*, 237–246.

(30) Dao Thi, H.; Djokic, M. R.; Van Geem, K. M. Detailed Group-Type Characterization of Plastic-Waste Pyrolysis Oils: By Compre-

hensive Two-Dimensional Gas Chromatography Including Linear, Branched, and Di-Olefins. *Separations* **2021**, *8* (7), 103.

(31) Hasan, M. M.; Rasul, M. G.; Jahirul, M. I.; Khan, M. M. K. Characterization of pyrolysis oil produced from organic and plastic wastes using an auger reactor. *Energy Conversion and Management* **2023**, *278*, No. 116723.

(32) Marshall, A. G.; Rodgers, R. P. Petroleumomics: The Next Grand Challenge for Chemical Analysis. *Acc. Chem. Res.* **2004**, *37* (1), 53–59.

(33) Chacón-Patiño, M. L.; Niles, S. F.; Marshall, A. G.; Hendrickson, C. L.; Rodgers, R. P. Role of Molecular Structure in the Production of Water-Soluble Species by Photo-oxidation of Petroleum. *Environ. Sci. Technol.* **2020**, *54* (16), 9968–9979.

(34) Chacón-Patiño, M. L.; Rowland, S. M.; Rodgers, R. P. Advances in Asphaltene Petroleumomics. Part 1: Asphaltenes Are Composed of Abundant Island and Archipelago Structural Motifs. *Energy Fuels* **2017**, *31* (12), 13509–13518.

(35) Podgorski, D. C.; Corilo, Y. E.; Nyadong, L.; Lobodin, V. V.; Bythell, B. J.; Robbins, W. K.; McKenna, A. M.; Marshall, A. G.; Rodgers, R. P. Heavy Petroleum Composition. 5. Compositional and Structural Continuum of Petroleum Revealed. *Energy Fuels* **2013**, *27* (3), 1268–1276.

(36) Mase, C.; Maillard, J. F.; Paupy, B.; Farenc, M.; Adam, C.; Hubert-Roux, M.; Afonso, C.; Giusti, P. Molecular Characterization of a Mixed Plastic Pyrolysis Oil from Municipal Wastes by Direct Infusion Fourier Transform Ion Cyclotron Resonance Mass Spectrometry. *Energy Fuels* **2021**, *35* (18), 14828–14837.

(37) Hassibi, N.; Quiring, Y.; Carré, V.; Aubriet, F.; Vernex-Loset, L.; Mauviel, G.; Burklé-Vitzthum, V. Analysis and control of products obtained from pyrolysis of polypropylene using a reflux semi-batch reactor and GC-MS/FID and FT-ICR MS. *Journal of Analytical and Applied Pyrolysis* **2023**, *169*, No. 105826.

(38) Ware, R. L.; Rowland, S. M.; Rodgers, R. P.; Marshall, A. G. Advanced Chemical Characterization of Pyrolysis Oils from Landfill Waste, Recycled Plastics, and Forestry Residue. *Energy Fuels* **2017**, *31* (8), 8210–8216.

(39) Ware, R. L.; Rowland, S. M.; Lu, J.; Rodgers, R. P.; Marshall, A. G. Compositional and Structural Analysis of Silica Gel Fractions from Municipal Waste Pyrolysis Oils. *Energy Fuels* **2018**, *32* (7), 7752–7761.

(40) Mase, C.; Maillard, J. F.; Paupy, B.; Hubert-Roux, M.; Afonso, C.; Giusti, P. Speciation and Semiquantification of Nitrogen-Containing Species in Complex Mixtures: Application to Plastic Pyrolysis Oil. *ACS Omega* **2022**, *7* (23), 19428–19436.

(41) Mase, C.; Maillard, J. F.; Piparo, M.; Friederici, L.; Rüger, C. P.; Marceau, S.; Paupy, B.; Hubert-Roux, M.; Afonso, C.; Giusti, P. GC-FTICR mass spectrometry with dopant assisted atmospheric pressure photoionization: application to the characterization of plastic pyrolysis oil. *Analyst* **2023**, *148* (20), 5221–5232.

(42) Dhahak, A.; Carre, V.; Aubriet, F.; Mauviel, G.; Burklé-Vitzthum, V. Analysis of Products Obtained from Slow Pyrolysis of Poly(ethylene terephthalate) by Fourier Transform Ion Cyclotron Resonance Mass Spectrometry Coupled to Electrospray Ionization (ESI) and Laser Desorption Ionization (LDI). *Ind. Eng. Chem. Res.* **2020**, *59* (4), 1495–1504.

(43) Lazzari, E.; Piparo, M.; Mase, C.; Levacher, L.; Stefanuto, P.-H.; Purcaro, G.; Focant, J.-F.; Giusti, P. Chemical elucidation of recycled plastic pyrolysis oils by means of GC × GC-PI-TOF-MS and GC-VUV. *Journal of Analytical and Applied Pyrolysis* **2023**, *176*, No. 106224.

(44) Ureel, Y.; Chacón-Patiño, M. L.; Kusenberg, M.; Rodgers, R. P.; Sabbe, M. K.; Van Geem, K. M. Characterization of PP and PE Waste Pyrolysis Oils by Ultrahigh-Resolution Fourier Transform Ion Cyclotron Resonance Mass Spectrometry. *Energy Fuels* **2024**, *38*, 11148.

(45) Rodgers, R. P.; Mapolelo, M. M.; Robbins, W. K.; Chacón-Patiño, M. L.; Putman, J. C.; Niles, S. F.; Rowland, S. M.; Marshall, A. G. Combating selective ionization in the high resolution mass spectral

- characterization of complex mixtures. *Faraday Discuss.* **2019**, *218*, 29–51.
- (46) Smith, D. F.; Podgorski, D. C.; Rodgers, R. P.; Blakney, G. T.; Hendrickson, C. L. 21 T FT-ICR Mass Spectrometer for Ultrahigh-Resolution Analysis of Complex Organic Mixtures. *Anal. Chem.* **2018**, *90* (3), 2041–2047.
- (47) Olcese, R.; Carré, V.; Aubriet, F.; Dufour, A. Selectivity of Bio-oils Catalytic Hydrotreatment Assessed by Petroleomic and GC*GC/MS-FID Analysis. *Energy Fuels* **2013**, *27* (4), 2135–2145.
- (48) Cho, Y.; Ahmed, A.; Islam, A.; Kim, S. Developments in FT-ICR MS instrumentation, ionization techniques, and data interpretation methods for petroleomics. *Mass Spectrom. Rev.* **2015**, *34* (2), 248–263.
- (49) Barrow, M. P.; Peru, K. M.; Headley, J. V. An Added Dimension: GC Atmospheric Pressure Chemical Ionization FTICR MS and the Athabasca Oil Sands. *Anal. Chem.* **2014**, *86* (16), 8281–8288.
- (50) Chacón-Patiño, M. L.; Moulian, R.; Barrère-Mangote, C.; Putman, J. C.; Weisbrod, C. R.; Blakney, G. T.; Bouyssiere, B.; Rodgers, R. P.; Giusti, P. Compositional Trends for Total Vanadium Content and Vanadyl Porphyrins in Gel Permeation Chromatography Fractions Reveal Correlations between Asphaltene Aggregation and Ion Production Efficiency in Atmospheric Pressure Photoionization. *Energy Fuels* **2020**, *34* (12), 16158–16172.
- (51) Nisson, D. M.; Walters, C. C.; Chacón-Patiño, M. L.; Weisbrod, C. R.; Kieft, T. L.; Sherwood Lollar, B.; Warr, O.; Castillo, J.; Perl, S. M.; Cason, E. D.; et al. Radiolytically reworked Archean organic matter in a habitable deep ancient high-temperature brine. *Nat. Commun.* **2023**, *14* (1), 6163.
- (52) Chacón-Patiño, M. L.; Rowland, S. M.; Rodgers, R. P. The Compositional and Structural Continuum of Petroleum from Light Distillates to Asphaltenes: The Boduszynski Continuum Theory As Revealed by FT-ICR Mass Spectrometry. In *The Boduszynski Continuum: Contributions to the Understanding of the Molecular Composition of Petroleum*; ACS Symposium Series, American Chemical Society: 2018, Vol. 1282, pp 113–171.
- (53) Chacón-Patiño, M. L.; Rowland, S. M.; Rodgers, R. P. Advances in Asphaltene Petroleomics. Part 2: Selective Separation Method That Reveals Fractions Enriched in Island and Archipelago Structural Motifs by Mass Spectrometry. *Energy Fuels* **2018**, *32* (1), 314–328.
- (54) Pudenzi, M. A.; Eberlin, M. N. Assessing Relative Electrospray Ionization, Atmospheric Pressure Photoionization, Atmospheric Pressure Chemical Ionization, and Atmospheric Pressure Photo- and Chemical Ionization Efficiencies in Mass Spectrometry Petroleomic Analysis via Pools and Pairs of Selected Polar Compound Standards. *Energy Fuels* **2016**, *30* (9), 7125–7133.
- (55) Abbas-Abadi, M. S.; Kusenber, M.; Zayoud, A.; Roosen, M.; Vermeire, F.; Madanikashani, S.; Kuzmanović, M.; Parvizi, B.; Kresovic, U.; De Meester, S.; Van Geem, K. M. Thermal pyrolysis of waste versus virgin polyolefin feedstocks: The role of pressure, temperature and waste composition. *Waste Management* **2023**, *165*, 108–118.
- (56) Abbas-Abadi, M. S.; Zayoud, A.; Kusenber, M.; Roosen, M.; Vermeire, F.; Yazdani, P.; Van Waeyenberg, J.; Eschenbacher, A.; Hernandez, F. J. A.; Kuzmanović, M.; et al. Thermochemical recycling of end-of-life and virgin HDPE: A pilot-scale study. *Journal of Analytical and Applied Pyrolysis* **2022**, *166*, No. 105614.
- (57) Wagner, J. R., Jr. *Multilayer flexible packaging*; William Andrew: 2016.
- (58) Kopinke, F. D.; Zimmermann, G.; Reyniers, G. C.; Froment, G. F. Relative rates of coke formation from hydrocarbons in steam cracking of naphtha. 2. Paraffins, naphthenes, mono-, di-, and cycloolefins, and acetylenes. *Ind. Eng. Chem. Res.* **1993**, *32* (1), 56–61.
- (59) Kopinke, F. D.; Zimmermann, G.; Reyniers, G. C.; Froment, G. F. Relative rates of coke formation from hydrocarbons in steam cracking of naphtha. 3. Aromatic hydrocarbons. *Ind. Eng. Chem. Res.* **1993**, *32* (11), 2620–2625.
- (60) Kopinke, F. D.; Zimmermann, G.; Nowak, S. On the mechanism of coke formation in steam cracking—conclusions from results obtained by tracer experiments. *Carbon* **1988**, *26* (2), 117–124.
- (61) Beyler, C. L.; Hirschler, M. M. *Thermal decomposition of polymers*; National Fire Protection Association Quincy: MA, 2002.
- (62) Lopez, G.; Olazar, M.; Aguado, R.; Elordi, G.; Amutio, M.; Artetxe, M.; Bilbao, J. Vacuum Pyrolysis of Waste Tires by Continuously Feeding into a Conical Spouted Bed Reactor. *Ind. Eng. Chem. Res.* **2010**, *49* (19), 8990–8997.
- (63) Klaimy, S.; Lamontier, J. F.; Casetta, M.; Heymans, S.; Duquesne, S. Recycling of plastic waste using flash pyrolysis – Effect of mixture composition. *Polym. Degrad. Stab.* **2021**, *187*, No. 109540.
- (64) Bagri, R.; Williams, P. T. Catalytic pyrolysis of polyethylene. *Journal of Analytical and Applied Pyrolysis* **2002**, *63* (1), 29–41.
- (65) Bolgar, M.; Hubball, J.; Groeger, J.; Meronek, S. *Handbook for the chemical analysis of plastic and polymer additives*; CRC Press: 2015.
- (66) Hahladakis, J. N.; Velis, C. A.; Weber, R.; Iacovidou, E.; Purnell, P. An overview of chemical additives present in plastics: Migration, release, fate and environmental impact during their use, disposal and recycling. *Journal of Hazardous Materials* **2018**, *344*, 179–199.
- (67) Pelzl, B.; Wolf, R.; Kaul, B. L. *Plastics, Additives*; Wiley-VCH Verlag GmbH & Co. KGaA Weinheim: Germany, 2018.
- (68) Ügdüler, S.; Van Geem, K. M.; Roosen, M.; Delbeke, E. I. P.; De Meester, S. Challenges and opportunities of solvent-based additive extraction methods for plastic recycling. *Waste Management* **2020**, *104*, 148–182.
- (69) Natta, G.; Pino, P.; Ercoli, R. Hydrogen Transfer Reactions Accompanying the Cobalt-catalyzed Addition of Carbon Monoxide to Olefinic Compounds. *J. Am. Chem. Soc.* **1952**, *74* (18), 4496–4498.
- (70) Chiusoli, G. P. Catalysis of olefin and carbon monoxide insertion reactions. *Acc. Chem. Res.* **1973**, *6* (12), 422–427.
- (71) Wu, X.-F.; Fang, X.; Wu, L.; Jackstell, R.; Neumann, H.; Beller, M. Transition-Metal-Catalyzed Carbonylation Reactions of Olefins and Alkynes: A Personal Account. *Acc. Chem. Res.* **2014**, *47* (4), 1041–1053.
- (72) Vasilio, A. K.; Kim, J. H.; Ormond, T. K.; Piech, K. M.; Urness, K. N.; Scheer, A. M.; Robichaud, D. J.; Mukarakate, C.; Nimlos, M. R.; Daily, J. W.; Guan, Q.; Carstensen, H. H.; Ellison, G. B. Biomass pyrolysis: thermal decomposition mechanisms of furfural and benzaldehyde. *J. Chem. Phys.* **2013**, *139* (10), 104310.
- (73) Furimsky, E. Catalytic hydrodeoxygenation. *Applied Catalysis A: General* **2000**, *199* (2), 147–190.
- (74) Rönkkö, H.-L.; Knuuttila, H.; Denifl, P.; Leinonen, T.; Venäläinen, T. Structural studies on a solid self-supported Ziegler–Natta-type catalyst for propylene polymerization. *J. Mol. Catal. A: Chem.* **2007**, *278* (1), 127–134.
- (75) Mokwena, K. K.; Tang, J. Ethylene vinyl alcohol: a review of barrier properties for packaging shelf stable foods. *Critical reviews in food science and nutrition* **2012**, *52* (7), 640–650.
- (76) Lange, J.; Wyser, Y. Recent innovations in barrier technologies for plastic packaging—a review. *Packaging Technology and Science: An International Journal* **2003**, *16* (4), 149–158.
- (77) Miller, K. S.; Krochta, J. M. Oxygen and aroma barrier properties of edible films: A review. *Trends in food science & technology* **1997**, *8* (7), 228–237.